

Wildfire-driven changes in the abundance of gas-phase pollutants in the city of Boise, ID during summer 2018



Emily Lill^{a,*}, Jakob Lindaas^a, Julieta F. Juncosa Calahorrano^a, Teresa Campos^b, Frank Flocke^b, Eric C. Apel^b, Rebecca S. Hornbrook^b, Alan Hills^b, Alex Jarnot^c, Nicola Blake^c, Wade Permar^d, Lu Hu^d, Andrew Weinheimer^b, Geoff Tyndall^b, Denise D.e Montzka^b, Samuel R. Hall^b, Kirk Ullmann^b, Joel Thornton^e, Brett B. Palm^{e,1}, Qiaoyun Peng^e, Ilana Pollack^a, Emily V. Fischer^a

^a Colorado State University, Department of Atmospheric Science, Fort Collins, CO, USA

^b Atmospheric Chemistry Observations & Modeling Laboratory, National Center for Atmospheric Research, Boulder, CO, USA

^c University of California Irvine, Department of Chemistry, Irvine, CA, USA

^d University of Montana, Department of Chemistry and Biochemistry, Missoula, MT, USA

^e University of Washington, Department of Atmospheric Science, Seattle, WA, USA

ARTICLE INFO

Keywords:
Wildfire
Emissions
Air quality
VOC

ABSTRACT

During summer 2018, wildfire smoke impacted the atmospheric composition and photochemistry across much of the western U.S. Smoke is becoming an increasingly important source of air pollution for this region, and this problem will continue to be exacerbated by climate change. The Western Wildfire Experiment for Cloud Chemistry, Aerosol Absorption and Nitrogen (WE-CAN) project deployed a research aircraft in summer 2018 (22 July – 31 August) to sample wildfire smoke during its first day of atmospheric evolution using Boise, ID as a base. We report on measurements of gas-phase species collected in aircraft ascents and descents through the boundary layer. We classify ascents and descents with mean hydrogen cyanide (HCN) > 300 pptv and acetonitrile (CH₃CN) > 200 pptv as smoke-impacted. We contrast data from the 16 low/no-smoke and 16 smoke-impacted ascents and descents to determine differences between the two data subsets. The smoke was transported from local fires in Idaho as well as from major fire complexes in Oregon and California. During the smoke-impacted periods, the abundances of many gas-phase species, including carbon monoxide (CO), ozone (O₃), formaldehyde (HCHO), and peroxyacetyl nitrate (PAN) were significantly higher than low/no-smoke periods. When compared to ground-based data obtained from the Colorado Front Range in summer 2015, we found that a similar subset of gas-phase species increased when both areas were smoke-impacted. During smoke-impacted periods, the average abundances of several Hazardous Air Pollutants (HAPs), including benzene, HCHO, and acetaldehyde, were comparable in magnitude to the annual averages in many major U.S. urban areas.

1. Introduction

Wildfire smoke is becoming an increasingly important source of air pollution for the western U.S. (O'Dell et al., 2019; McClure and Jaffe, 2018b; Laing and Jaffe, 2019), and this problem is likely to be exacerbated by climate change (Ford et al., 2018; Liu et al., 2016; Brey et al., 2021; Abatzoglou and Williams, 2016; Harvey, 2016; Yue et al., 2013). Western U.S. wildfires produce large emission fluxes of many pollutants

(Wiedinmyer et al., 2006) including fine particulate matter (Garofalo et al., 2019; Liu et al., 2017; Palm et al., 2020), a suite of volatile organic compounds (VOCs; Permar et al., 2021) including hazardous air pollutants (HAPs; O'Dell et al., 2020), and reactive nitrogen (Lindaas et al., 2021b). The composition of wildfires smoke evolves over time, and there is often substantial production of secondary pollutants (e.g., ozone (O₃) and acyl peroxy nitrates (APNs)) (Juncosa Calahorrano et al., 2020; Jaffe and Wigder, 2012). As wildfires become more prevalent,

Peer review under responsibility of Turkish National Committee for Air Pollution Research and Control.

* Corresponding author. Colorado State University, Department of Atmospheric Science, 3915 Laporte Ave, Fort Collins, CO, 80521, USA.

E-mail address: emily.lill@colostate.edu (E. Lill).

¹ Now at: Atmospheric Chemistry Observations & Modeling Laboratory, National Center for Atmospheric Research, Boulder, CO.

understanding their effects on air quality is becoming increasingly important (Val Martin et al., 2015; Jaffe et al., 2020).

The Western Wildfire Experiment for Cloud Chemistry, Aerosol Absorption and Nitrogen (WE-CAN) project deployed the National Science Foundation/National Center for Atmospheric Research (NSF/NCAR) C-130 research aircraft in summer 2018 (22 July – 31 August) to sample wildfire smoke (Lindaas et al., 2021b; Juncosa Calahorrano et al., 2020; Palm et al., 2020; Peng et al., 2020). Boise, ID is routinely impacted by smoke from both fires in Idaho and major fire complexes in other regions (Brey et al., 2018), and this smoke substantially degrades local air quality (McClure and Jaffe, 2018b; Fowler, 2019). The summer 2018 wildfire season was particularly severe, with the highest suppression costs in prior history and some of the highest fine particulate matter concentrations ever observed in many western U.S. cities (Jaffe et al., 2020). Fig. 1 provides an example of visibility impacts in Boise, ID caused by wildfire smoke during the WE-CAN study period. On July 24, 2018, Boise was impacted by smoke from large wildfires in southwestern Oregon. Fig. 1c shows smoke plume polygons from the National Oceanic and Atmospheric Administration (NOAA) Hazard Mapping System (HMS) Fire and Smoke Product for July 24, 2018 (Brey et al., 2018; Rolph et al., 2009; Ruminski et al., 2006). Here we present measurements of a suite of gas-phase species collected in NSF/NCAR C-130 ascents and descents through the Boise, ID boundary layer during the summer 2018 WE-CAN study period. We identify ascents and descents that are smoke-impacted and identify changes in composition associated with the presence of wildfire smoke. This analysis is different from most other studies focused on the impact of wildfire smoke on air quality in western U.S. urban areas because our analysis extends beyond criteria pollutants. Most prior studies have focused on the impact of smoke on fine particulate matter or O₃ abundances due to the available data.

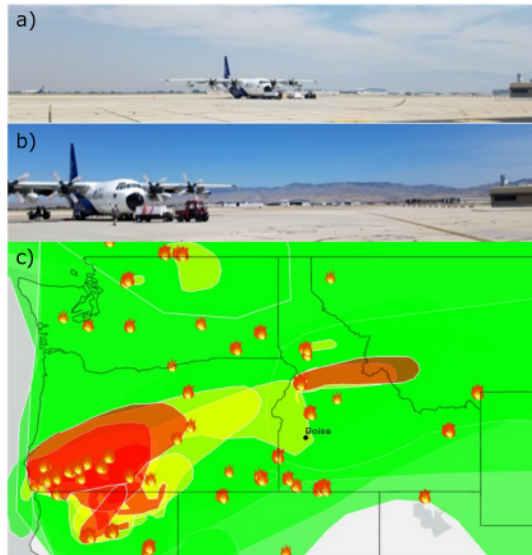


Fig. 1. a) Photograph of the Boise Mountains from Boise Airport on an example of a smoke-impacted day (July 24, 2018). b) Photograph of the Boise Mountains from Boise Airport on an example low/no-smoke day (August 03, 2018). c) NOAA Hazard Mapping System (HMS) smoke plumes and smoke-producing wildfires for July 24, 2018. See Brey et al. (2018) and Ruminski et al. (2006) for a description of these datasets. The green, yellow, orange and red shading qualitatively indicate the presence of dilute ($5 \mu\text{g m}^{-3} \text{ PM}_{2.5}$), concentrated, more concentrated ($16 \mu\text{g m}^{-3} \text{ PM}_{2.5}$), and very concentrated ($27 \mu\text{g m}^{-3} \text{ PM}_{2.5}$) smoke plumes in the atmospheric column identified by HMS analysis.

2. Methods

2.1. WE-CAN data collection

During WE-CAN, the NSF/NCAR C-130 research aircraft was outfitted with a large set of trace gas and aerosol measurements optimized for sampling wildfire smoke composition. Details of the 2018 WE-CAN field campaign and relevant airborne instrumentation used in this analysis can be found in Lindaas et al. (2021a), Permar et al. (2021), and on the WE-CAN project website (https://www.eol.ucar.edu/field_projects/we-can). Boise, ID was selected as the project base of operations for the aircraft owing to its centralized location and close proximity to areas with prominent wildfire activity in the western U.S. during summertime. The aircraft flew 16 research flights (i.e., 32 total ascents and descents) while stationed at Boise Airport (KBOI; 43.5658° N, 116.2223° W, elev = 0.875 km above mean sea level) between 24 July and August 31, 2018, and sampled fresh smoke from more than 20 major wildfires throughout the western U.S. (Lindaas et al., 2021b; Permar et al., 2021; Barry et al., 2021; Juncosa Calahorrano et al., 2021; Palm et al., 2020; O'Dell et al., 2020; Peng et al., 2020). Research flights typically took off from KBOI between 12:00 and 14:00 mountain daylight saving time (MDT) and landed between 19:00 and 21:00 MDT. Data collected during each ascent out of and descent into KBOI provide an opportunity to evaluate smoke-impacted and low/no-smoke periods in Boise. For this analysis, we consider the mean of a variable within the boundary layer (see Section 2.3) as a single sample. This means that there are 32 samples for each variable. These data are then subset into smoke-impacted versus low/no-smoke conditions as described in Section 2.4. Differences between means of these two subsets of data are tested using a student's t-test. Significance is reported at the 95% confidence level.

2.2. Airborne measurements

Measurements used in this analysis are briefly described below. Further details can be found in Lindaas et al. (2021a) and Permar et al. (2021). State parameter, 1-Hz navigation, and microphysics flight-level data from the C-130 aircraft are available from <https://data.eol.ucar.edu/dataset/548.005>. Key measurement details regarding measured species, instrument/technique, and detection limit with uncertainty can be found in Table S1.

2.2.1. O₃ and CO

O₃ was measured with an NCAR single-channel chemiluminescence instrument (Ridley et al., 1992; Ridley and Graheck, 1990). These data have a precision of <1 ppbv with a 1 s temporal resolution and an accuracy of ± 1 ppbv or 2% (whichever is greater) for O₃.

CO was measured with a commercial Mini-TILDAS tunable diode laser infrared absorption spectrometer (Aerodyne Research) (Lebegue et al., 2016). These data have a precision of 100 ppt with a 2-s temporal resolution and an accuracy of ± 0.6 ppbv for CO. A Picarro G-2401-m analyzer was used for the measurement of CO₂ and CH₄, which also provided an additional, but lower precision, measurement of CO.

2.2.2. Oxidized nitrogen species

Gaseous hydrogen cyanide (HCN) and nitric acid (HNO₃) were measured by the University of Washington high-resolution chemical ionization time-of-flight mass spectrometer using iodide-adduct ionization (I⁻-CIMS; Lee et al., 2014; Peng et al., 2020; Palm et al., 2020). Ambient air was sampled at 20 lpm through a straight ~50-cm length, 0.75-in OD PTFE Teflon tube. Juncosa Calahorrano et al. (2021) and Lindaas et al. (2021a) contain detailed explanations of the instrument's operation.

Peroxacetyl nitrate (PAN) and propionyl peroxy nitrite (PPN) were measured with a thermal dissociation chemical ionization mass spectrometer (CIMS) (Slusher et al., 2004; Zheng et al., 2011). Accuracy is $\pm 12\%$ or 25 pptv (whichever is greater) for PAN and PPN, and precision

is ± 20 pptv on average across the flight. Please see further details in Juncosa Calahorrano et al. (2021) and Lindaas et al. (2021a).

2.2.3. Photolysis frequencies

Photolysis frequencies were calculated from spectrally resolved (290–680 nm) actinic flux density measurements from the High-performance Instrumented Airborne Platform for Environmental Research (HIAPER) Airborne Radiation Package – Actinic Flux (HARP-Actinic Flux) instrument (Hall et al., 2018).

2.2.4. NMVOCs

The University of Montana proton-transfer-reaction time-of-flight mass spectrometer (PTR-ToF-MS 4000, Ionicon Analytik, Innsbruck, Austria) made 2–5 Hz NMVOC measurements, including acetonitrile (CH_3CN). The PTR-ToF-MS is custom-built into a standard NSF/NCAR HIAPER Gulfstream-V (GV) rack with the mass spectrometer vibration damped separately. Permar et al. (2021) provides a robust description of the PTR-ToF-MS used in WE-CAN. There were 121 VOCs reported in the publicly available dataset for the PTR.

VOCs were also measured using NCAR Trace Organic Gas Analyzer (TOGA; Apel et al., 2015). During WE-CAN, TOGA had a sample collection time of 28 s every 100 s for the first 11.5 research flights, and then transitioned to a 33 s sampling time every 105 s for the remainder of the research flights. The following TOGA measurements (uncertainties and detection limits in parentheses) were used to identify smoke-impacted observations, the chemical aging of those smoke-impacted observations, and as anthropogenic tracers: HCN (20%, 5 ppt), acetonitrile (CH_3CN ; 40%, 10 ppt), 2-methylfuran (20%, 5 ppt), acrolein (30%, 0.5 ppt), acrylonitrile (50%, 1 ppt), 2,2,4-trimethylpentane (15%, 0.5 ppt), tetrachloroethene (15%, 0.5 ppt), chloroform (15%, 2 ppt), HFC-134a (50%, 1 ppt), and HCFC-22 (50%, 1 ppt). There were 69 VOCs reported in the publicly available dataset for TOGA.

2.3. Boundary layer identification

We identify the top of the boundary layer using potential temperature (K) profiles collected during ascents and descents out of and into KBOI. The top of the boundary layer is signified by a sharp increase in the potential temperature gradient, which indicates the transition to a more stable layer (Cazorla and Juncosa, 2018). Fig. 2 demonstrates this for an example ascent and descent where the boundary layer was visually identified by the abrupt change in slope. The boundary layer varied in height from 0.9 km to 2.7 km above ground level throughout the sampled ascents and descents.

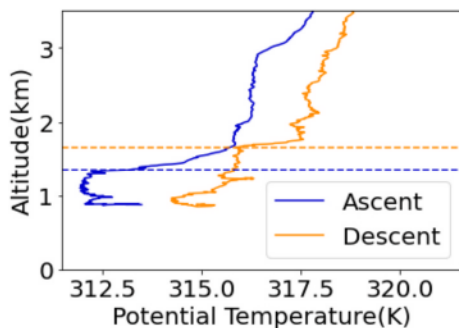


Fig. 2. Measured potential temperature (K) and altitude (km) for the ascent (blue) from and descent into Boise, ID (orange) of the NSF/NCAR C-130 on August 15, 2018. Dashed lines signify the top of the boundary layer for the ascent (1.34 km) and descent (1.65 km), identified by the presence of an abrupt change in potential temperature.

2.4. Smoke identification

We classify an ascent or descent as smoke-impacted when the mean HCN mixing ratio is > 300 ppt or the mean acetonitrile (CH_3CN) is > 200 ppt. HCN and CH_3CN are commonly used as tracers of smoke-impacted because biomass burning is their dominant source, and they have long (i.e., months to years) atmospheric lifetimes (de Gouw et al., 2003; Li et al., 2000, 2003). Despite HCN being used as a tracer of biomass burning, there are some limitations associated with the species. There is a large variability in HCN emission factors within the same fire type (Akagi et al., 2011), and there can be large differences in the enhancement of HCN relative to CO (i.e., $\Delta\text{HCN}/\Delta\text{CO}$) between fires (Akagi et al., 2011). Combined, these two factors can complicate attribution of smoke in regions impacted by multiple types of biomass burning. CH_3CN mixing ratio values may also have interference from anthropogenic sources (Huangfu et al., 2021). However, the lifetime of HCN and CH_3CN against atmospheric sinks (reaction with OH or O (^1D), photolysis, and scavenging by precipitation) are long, on the scale of a few years (Li et al., 2003), thus these species are essentially conserved relative to CO on the timescales relevant for smoke-transport to Boise in summer 2018. We determined the cut-off values of HCN and CH_3CN by plotting histograms of the two species (Fig. S1). For each histogram, there were two modes, representing smoke-impacted and low/no-smoke conditions. We assigned a cut-off value based on the division between the two modes. Based on this criteria, 16 ascents and descents are classified as smoke-impacted and 16 ascents and descents are classified as low/no-smoke. Please note that our low/no-smoke criteria is not strictly smoke-free. Due to the ubiquitous nature of the 2018 wildfire season, even when the ascents/descents through the boundary layer at Boise were classified as “low/no-smoke” based on trace gas composition, the NOAA HMS Fire and Smoke Product indicated that there were elevated levels of smoke aloft with the exception of the ascent on August 28, 2018.

The flight paths of smoke-impacted and low/no-smoke ascents and descents are shown in Fig. 3a. These maps reflect the common arrival and departure corridors for KBOI. Both categories were associated with similar flight paths. Wind speeds and directions for smoke-impacted and low/no-smoke ascents and descents are shown in Fig. 3b. On average,

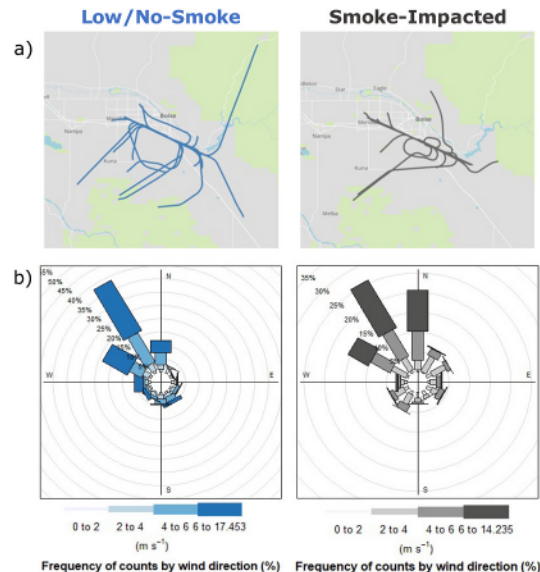


Fig. 3. (a) Flight tracks associated with low/no-smoke (blue; left) and smoke-impacted (grey; right) ascents out of and descents into KBOI. (b) Wind speeds and directions of smoke-impacted (blue; left) and low/no-smoke (grey; right) ascents and descents. The percentages indicate the frequency of counts by wind direction. The shading represents intervals of increasing wind speed.

winds for both conditions were northwesterly, and there were no major differences in wind conditions during smoke-impacted versus low/no-smoke conditions. There is no significant difference in mean ambient temperature between the two subsets of data.

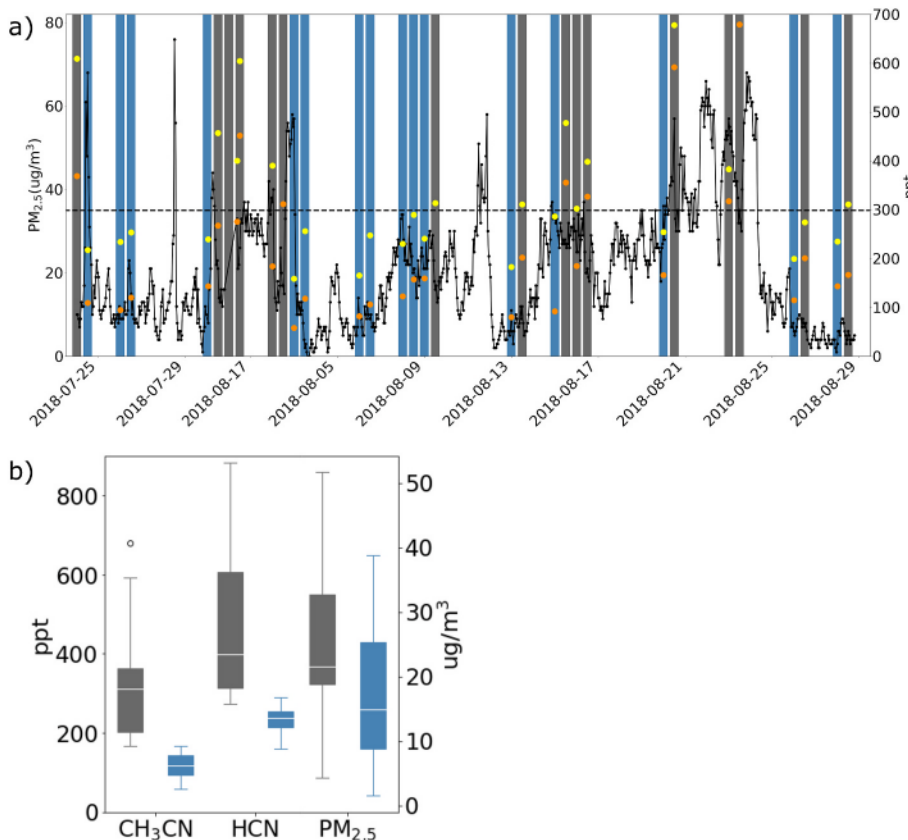
While there were many fires active within Idaho during summer 2018, smoke impacting Boise often traveled from the west from wildfires burning in Washington, California, and Oregon. Thus, the age of the smoke plumes was often >1 day (O'Dell et al., 2020). Table S2 shows the likely primary source(s) of the smoke in Boise as determined by the NOAA HYSPLIT trajectory model and InciWeb reports.

3. Results and discussion

3.1. Surface $\text{PM}_{2.5}$ during smoke-impacted conditions

Elevated surface concentrations of fine particulate matter are expected in the presence of wildfire smoke, and these are often used along with satellite observations to indicate whether smoke is indeed impacting a surface monitoring site versus remaining aloft (e.g. McClure and Jaffe, 2018b; Brey et al., 2018; O'Dell et al., 2019; Magzamen et al., 2021). Fig. 4a presents a time series of surface $\text{PM}_{2.5}$ at the St. Luke's Meridian monitoring station (43.6°N , 116.3°W) west of downtown Boise. This figure shows that increased concentrations of $\text{PM}_{2.5}$ at the ground are associated with smoke-impacted ascents and descents. The average surface $\text{PM}_{2.5}$ on days with smoke-impacted (low/no-smoke) ascents or descents is $26 \mu\text{g m}^{-3}$ ($17 \mu\text{g m}^{-3}$). Despite the significant increases of $\text{PM}_{2.5}$ at 95% confidence, many of the smoke-impacted days were still below the EPA 24-h primary standard for $\text{PM}_{2.5}$ of $35 \mu\text{g m}^{-3}$. Since Boise is an urban area, elevated $\text{PM}_{2.5}$ levels were sometimes present on low/no smoke days due to other urban sources. The boxplots in

Fig. 4b shows the different distribution HCN and CH_3CN under smoke-impacted and low/no-smoke conditions.



3.2. Changes in gas-phase composition during smoke-impacted periods

CO is a product of incomplete combustion, and wildfires are a large source of CO on a global scale (van der Werf et al., 2017). The lifetime of CO in summer over continental regions is approximately 10 days (Holloway et al., 2000). We observed the mean CO in the Boise boundary layer to be elevated when impacted by smoke; the average CO mixing ratios in the smoke-impacted and low/no-smoke data subsets are 265 ppb and 150 ppb respectively, as shown in Fig. 5. Increased abundances of CO have been documented in other urban areas impacted by wildfire smoke. Lindaas et al. (2021a) documented a significant increase of 223

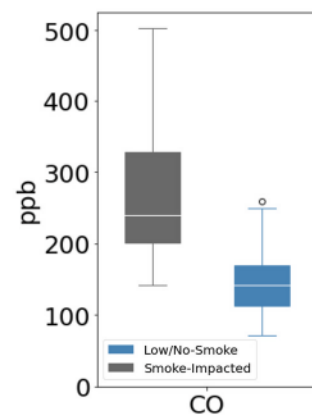


Fig. 5. Boxplot of the CO distributions observed in the boundary layer over Boise under smoke-impacted (grey) and low/no-smoke (blue) conditions. The white line in the boxes represents the median, the whiskers represent the 5th and 95th percentiles, and the black point is an outlier (1.5 times the interquartile range). See Table S3 for a summary of mean values.

Fig. 4. (a) Time series showing Air Quality System (AQS) surface data from Boise, ID from July 25, 2018 to August 30, 2018. Blue and grey lines represent low/no-smoke and smoke-impacted ascents out of and descents into Boise with the NSF/NCAR C-130 aircraft. The areas of no blue or grey lines (i.e. white space) are days when no research flight was conducted. The orange (yellow) points represent average CH_3CN (HCN) mixing ratios in the boundary layer measured by the C-130. The dashed line at $35 \mu\text{g m}^{-3}$ represents the EPA 24-h primary standard for $\text{PM}_{2.5}$. (b) Boxplots of CH_3CN , HCN, and $\text{PM}_{2.5}$ distributions observed in the boundary layer over Boise under smoke-impacted (grey) and low/no-smoke (blue) conditions. The white line in the boxes represents the median, the whiskers represent the 5th and 95th percentiles, and the black point is an outlier (1.5 times the interquartile range). Fig. 4b is the first in a series of figures that shows relationships between mixing ratios of various species during no/low smoke and smoke-impacted period. Table S3 includes the mean values, and significance associated with all these comparisons.

ppbv mean CO during July and 92 ppbv during August across the diurnal cycle during smoke-impacted periods compared to smoke-free periods during summer 2015 in the Colorado Front Range. CO mixing ratios increased in lockstep with $\text{PM}_{2.5}$ when aged smoke plumes passed through their study region.

3.3. Reactive nitrogen species

PAN, PPN, and HNO_3 are some of the oxidation products of NO_x that are formed rapidly in wildfire smoke plumes (Alvarado et al., 2010; Akagi et al., 2011; Liu et al., 2016; Juncosa Calahorrano et al., 2020; Lindaas et al., 2021b). During smoke-impacted periods in Boise, mean PAN (PPN) was 40% (66%) higher than during the low/no-smoke periods. Lindaas et al. (2021a) also observed consistently elevated PAN and PPN abundances across the day during smoke-impacted periods in the Front Range. At their study site, the average enhancements were 183 and 22 pptv respectively, approximately a 100% increase for both species. Mean August surface temperature in Boise in 2018 was 306 K versus 296 K in Erie, CO during 2015, the location of the Lindaas et al. (2021a) observations (National Weather Service). The two analyses are notably different in another important way. Lindaas et al. (2021a) compares PAN abundances throughout the full diurnal cycle, while this dataset was collected in the afternoon and early evening. This might also explain the lower relative PAN enhancement observed in Boise compared to Colorado. An additional factor is that the smoke could be of different ages or from fires with different emissions of reactive oxidized nitrogen (Lindaas et al., 2021b). Singh et al. (2010) also report a PPN/PAN of 0.10 (± 0.01) and 0.11 (± 0.02) for smoke intercepted below 3 km in the California Central Valley during the Arctic Research of the Composition of the Troposphere from Aircraft and Satellites (ARC-TAS-CARB). This is slightly lower than the ratios reported by Lindaas et al. (2021a) and this study of 0.14 and 0.17 for low/no-smoke and smoke-impacted periods. The PPN/PAN ratio also depends on the original composition of precursor gases, and these regions have different dominant anthropogenic emission profiles and biogenic emission rates.

As shown in Fig. 6, HNO_3 did not significantly change between the two periods. Lindaas et al. (2021a) also noted no change in HNO_3 between smoke-impacted and low/no-smoke periods. Many other studies have also shown that HNO_3 does not correlate with elevated CO in either fresh or aged smoke plumes (e.g., Yokelson et al., 2009; Alvarado et al., 2010; Liu et al., 2016; Akagi et al., 2011). Juncosa Calahorrano et al. (2021) provides a summary of the NO_y in fresh and aged smoke plumes sampled during WE-CAN. The observations suggest that HNO_3 accounts for $\sim 60\%$ of the total NO_y measured in smoke mixed with urban emissions and smoke intercepted below 3 km. Juncosa Calahorrano et al. (2021) excluded samples taken over the California Central Valley and Boise, Idaho in their analysis. The observed high percentage of HNO_3 to NO_y observed during WE-CAN is consistent with the smoke-impacted

data for Boise, where the average PAN to HNO_3 ratio is only 0.42. Singh et al. (2010) also reported a large contribution (40%) of HNO_3 to total NO_y during the ARCTAS-CARB campaign smoke-impacted observations over the California Central Valley. We are not able to conduct a similar comparison for total nitrate (i.e., gas HNO_3 and aerosol NO_3^-) because the aerosol mass spectrometer (AMS) on board the NSF/NCAR C-130 during WE-CAN was not collecting observations during the ascent and decent periods.

3.4. O_3 and NO_2 photolysis frequencies

Mean mixing ratios of O_3 were significantly higher (~ 13 ppb) in Boise during smoke-impacted periods (Fig. 7). O_3 is a secondary pollutant with a lifetime of ~ 5 days in the Intermountain West (Lu et al., 2016). While wildfires are a source of tropospheric O_3 , O_3 production in wildfire smoke is not fully understood (Jaffe and Wigder, 2012) and can vary substantially with emissions, dilution rates, and other factors (Gong et al., 2017). Our observations are consistent with a previous study showing O_3 enhancements during smoke-impacted days in Boise from 2006 to 2017 (McClure and Jaffe, 2018b), as well as the U.S.-wide analysis of Brey et al. (2021). McClure and Jaffe (2018b) found that when PM is very elevated, O_3 mixing ratios plateau or decline in Boise. The pattern is not present in the small subset of data we show here (see Fig. S2). The slope of our O_3/CO regression line is 0.06 which falls within the values presented by Jaffe and Wigder (2012) for the $\leq 1\text{--}2$ days plume age category. Lindaas et al. (2021a) also demonstrated higher O_3 mixing ratios during smoke-impacted periods in the Colorado

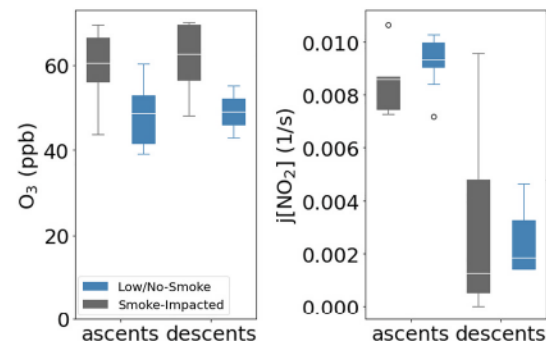


Fig. 7. Boxplots of (a) O_3 and (b) NO_2 photolysis frequency distributions observed in the boundary layer over Boise under smoke-impacted (grey) and low/no-smoke (blue) conditions separated by ascents and descents. The white line in the boxes represents the median, the whiskers represent the 5th and 95th percentiles, and the points are the outliers (1.5 times the interquartile range). See Table S3 for a summary of mean values.

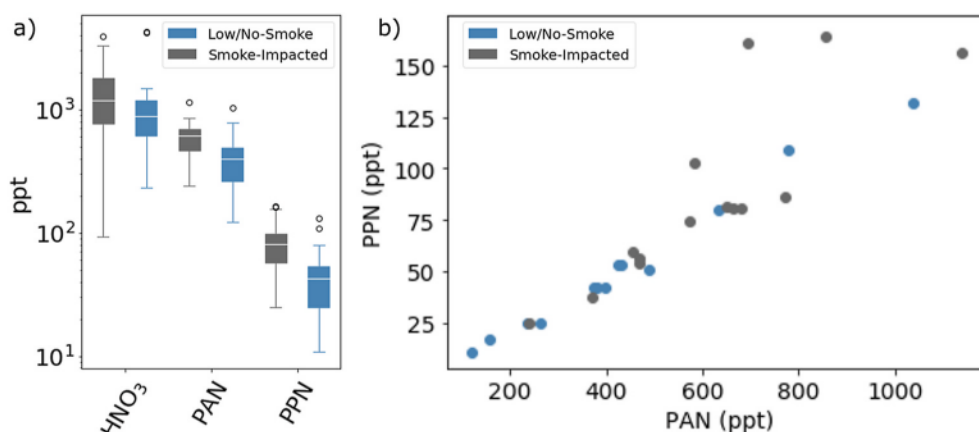


Fig. 6. (a) Boxplots of HNO_3 , PAN, and PPN distributions observed in the boundary layer over Boise under smoke-impacted (grey) and low/no-smoke (blue) conditions. The white line in the boxes represents the median, the whiskers represent the 5th and 95th percentiles, and the points are outliers (1.5 times the interquartile range). (b) Correlation of observed PPN and PAN in the boundary layer over Boise in smoke-impacted (grey) and "low/no smoke" (blue) conditions. See Table S3 for a summary of mean values.

Front Range for a given temperature. During our study period, temperature is not significantly different between the smoke-impacted and low/no-smoke periods.

The “odd oxygen” (O_3) chemical family can be defined to include O_3 and minor species with which it cycles. Photolysis of NO_2 dominates O_3 production in the troposphere, and thus O_3 and NO_2 are often examined together. Here, we cannot specifically quantify changes in NO or NO_2 because these measurements were not reported during aircraft takeoff and landing periods. However, we can examine differences in the photolysis frequency of NO_2 (J NO_2). The mean J NO_2 decreased by 37% during smoke-impacted periods. We also examined NO_2 photolysis rates in the ascents and descents separately. The mean photolysis frequency of NO_2 was higher during ascents than descents because the ascents primarily occurred from midday to early afternoon (11:41 MST - 15:00 MST) while the descents were typically late afternoon to early evening (15:48 MST - 20:43 MST). Lindaas et al. (2021a) hypothesized a reduction in J NO_2 could have contributed to observed increases in NO_2 in the morning and evening of smoke-impacted periods in the Colorado Front Range. They did not measure actinic flux as part of that experiment, and our dataset does not quantify NO_x over Boise so our ability to test this hypothesis directly is limited.

3.5. NMVOCs

Fig. 8 presents boxplots of the distribution of VOCs in the smoke-impacted and low/no-smoke datasets, grouped by mean abundance. The mean abundances of most VOCs are higher during smoke-impacted periods, but 95% statistically-significant enhancements (denoted by *) are largely associated with VOCs with lifetimes longer than the transport time of the smoke (>1 day; e.g., propane and benzene) or VOCs with substantial secondary production (e.g., acetaldehyde).

The mean abundances of acetone, methyl ethyl ketone (MEK), acetaldehyde, and formaldehyde (HCHO) are higher in the smoke-impacted periods. These species are among the most abundant non-methane organic carbon (NMOC) species emitted from wildfires (Liu et al., 2017; Permar et al., 2021), and they are also produced secondarily in smoke plumes (Jost et al., 2003; Trentmann et al., 2003). Acetone and MEK have longer lifetimes (i.e., days to weeks) against oxidation by OH and photolysis (Atkinson et al., 2006; Brewer et al., 2019). The principal sink of acetaldehyde in smoke plumes is likely reaction with OH, with a lifetime on the order of 5 h (Atkinson et al., 2006). Photolysis is an additional slower sink on the order of a few days (Sander et al., 2006). The lifetime of HCHO against these two sinks is shorter, on the order of hours (Pope et al., 2005).

The mean mixing ratios of five hazardous air pollutants (HAPs) were determined to be significantly higher according to a student's t-test at

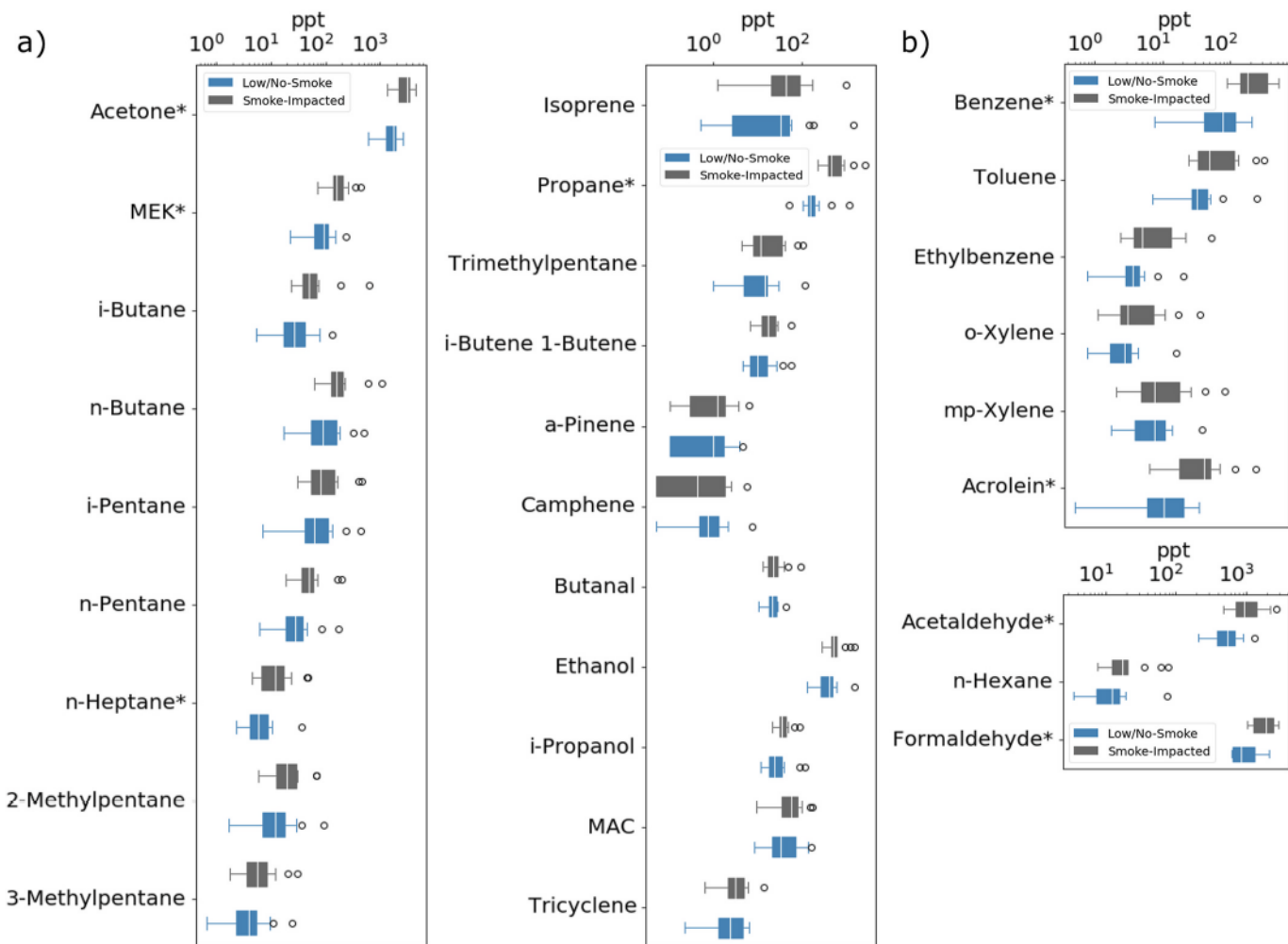


Fig. 8. Boxplots of many (a) non-HAPs and (b) HAPs NMVOCs distributions observed in the boundary layer over Boise under smoke-impacted (grey) and low/no-smoke (blue) conditions. The white line in the boxes represents the median, the whiskers represent the 5th and 95th percentiles, the black points are outliers (1.5 times the interquartile range), and * represents 95% statistical significance between the smoke-impacted and low/no-smoke impacted median values. See Table S3 for a summary of mean values.

95% confidence when Boise was smoke-impacted: benzene (174% higher), acrolein (238% higher), acetaldehyde (103% higher), HCHO (84% higher), and HCN (92% higher). Elevated benzene and acetaldehyde mixing ratios have been noted at other smoke-impacted locations (Wentworth et al., 2018).

Using the full WE-CAN dataset, O'Dell et al. (2020) showed that benzene, acrolein, acetaldehyde, HCHO, and HCN likely pose the largest gas-phase HAPs health risk in smoke. Each of these species has different atmospheric lifetimes, thus concentrations evolve in smoke plumes differently for each species. The smoke that was present in Boise ranged in age from approximately 1 to 3 days, as estimated using Hybrid Single-Particle Lagrangian Integrated Trajectory model (HYSPLIT) trajectory simulations (see Table S2 and associated methods in the SI). O'Dell et al. (2020) presented ratios of HAPs to sub-micron fine particulate matter (PM_{1}) in wildfire smoke because fine particulate matter is typically used as a smoke tracer in epidemiology studies of smoke exposure. Here, we compare ratios of HAPs to $PM_{2.5}$ observed during smoke-impacted periods in Boise. To compare HAPs to $PM_{2.5}$ ratios in Boise to those reported in O'Dell et al. (2020), which are to PM_{1} mass from the aircraft observations, we assume mass contribution from smoke particles with diameters between 1 and 2.5 μm is negligible. Bian et al. (2019) indicate particles of diameter 1–2.5 μm contribute <5% of total $PM_{2.5}$ vol in smoke. The mean ratio of HAPs to $PM_{2.5}$ in smoke-impacted air over Boise for acetaldehyde, acrolein, benzene, and formaldehyde, respectively, was 0.0819, 0.0046, 0.0295, and 0.0914. The median ratios of acetaldehyde, acrolein, benzene, and formaldehyde to PM_{1} of smoke 1–3 days old, as reported by O'Dell et al. (2020), were 0.0679, 0.0051, 0.0326, and 0.1209. With the exception of acetaldehyde, the HAPs to PM_{1} ratios in O'Dell et al. (2020) were slightly higher than the HAPs to $PM_{2.5}$ ratios in Boise. The mean abundances of toluene, ethylbenzene, xylene, and n-hexane were all higher during smoke-impacted periods, but these differences were not significant. This is likely due to both their shorter atmospheric lifetimes and contributions from anthropogenic sources in the Boise region.

Fig. 9 compares the concentration of HAPs when Boise was low/no-smoke and smoke-impacted to mean concentrations across select U.S. urban areas (Strum and Scheffe, 2016). The average amount of benzene, HCHO, and acetaldehyde on a smoke-impacted summer afternoon is comparable in magnitude to the annual average amounts in many larger urban areas across the U.S.

Lindaas et al. (2021a) presents the impact of aged wildfire smoke on atmospheric composition in the Colorado Front Range using data from summer 2015. Pollack et al. (2021) investigates the impact of wildfire smoke on O_3 and its precursors in Boulder County from 2017 to 2019. Lastly, McClure and Jaffe (2018a) examine high- O_3 events resulting from wildfire smoke in Boise during 2017. Fig. S3 compares the change in the smoke-impacted vs. low/no-smoke mean of many gas-phase

species in Boise to that previously documented in these studies. In Boise, there is a much larger relative change in the concentrations of the gas-phase species than in the Front Range and Boulder County during smoke-impacted periods. There are multiple potential explanations for the observed difference between these locations. The first is that the Front Range is generally more influenced by anthropogenic pollution sources than Boise. During low/no-smoke days, the mixing ratios of acetaldehyde, acetone, benzene, toluene, ethylbenzene, o-xylene, and isoprene were 226%, 81%, 128%, 524%, 738%, 1396%, and 51% higher respectively in the Colorado Front Range (Abeleira et al., 2017) than during low/no-smoke days in summer 2015. The region is influenced by emissions from oil and gas development in addition to traffic and industrial sources (Abeleira et al., 2017; Pollack et al., 2021; (Gilman et al., 2013). Another explanation for the larger relative enhancements in Boise is that Boise was located closer to major wildfires in 2018 than the Front Range in 2015.

4. Conclusions

Here we report on measurements of gas-phase species collected in aircraft ascents and descents through the Boise, ID boundary layer. We classify ascents and descents as smoke-impacted or low/no-smoke using HCN and CH_3CN , two long-lived tracers of biomass burning. The smoke was transported to Boise from both local fires in Idaho as well as from major fire complexes in Oregon and California. These measurements are unique because of their detailed composition information.

During the smoke-impacted periods, we observed a significant increase in CO and VOCs with lifetimes longer than the transport time of the smoke or significant secondary production. The mean mixing ratios of five HAPs increased significantly when Boise was smoke-impacted, pushing the concentrations of HAPs in Boise during smoke-impacted periods up to typical average concentrations in other substantially larger U.S. urban areas. Consistent with prior studies in the region, when Boise was impacted by smoke, there was a significant increase in the mean mixing ratios of O_3 , PAN, and PPN. We also observed a decrease in j_{NO_2} .

Wildfire smoke during 2018 impacted the atmospheric composition and photochemistry across much of the U.S. Mountain west. Wildfire smoke is becoming an increasingly important source of air pollution for the western U.S., and declines in air quality, such as those reported here, are likely to be exacerbated by climate change.

Data availability

Data used in this study are publicly available at https://data.eol.ucar.edu/master_lists/generated/we-can/ and https://aqs.epa.gov/aqsweb/airdata/download_files.html#Meta.

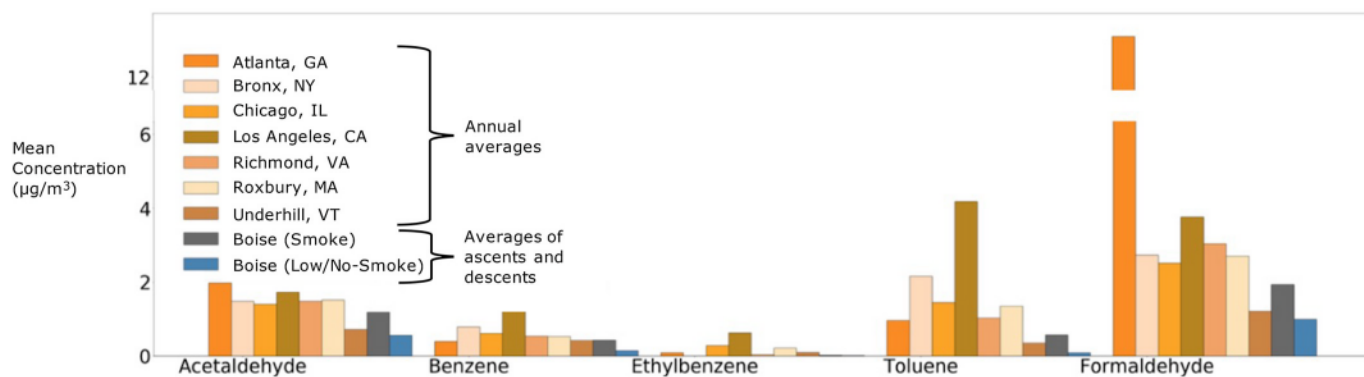


Fig. 9. Mean concentration of acetaldehyde, benzene, ethylbenzene, toluene, and formaldehyde in various U.S. cities (orange colors) as well as averages concentrations of these species measured during ascents and descents into or out of Boise on low/no-smoke (blue) and smoke-impacted days (grey). See Table S3 for a summary of mean values.

Credit author statement

Emily Lill: Conceptualization, Methodology, Formal analysis, Validation, Writing – original draft, Visualization, **Jakob Lindaas:** Conceptualization, Methodology, Investigation, Writing – review & editing, **Julieta F. Juncosa Calahorrano:** Conceptualization, Methodology, Investigation, Writing – review & editing, **Teresa Campos:** Investigation, Writing – review & editing, Resources, Data curation, **Frank Flocke:** Investigation, Writing – review & editing, Resources, Data curation, **Eric C. Apel:** Investigation, Writing – review & editing, Resources, Data curation, **Rebecca S. Hornbrook:** Investigation, Writing – review & editing, Resources, Data curation, **Alan Hills:** Investigation, Resources, Data curation, **Alex Jarnot:** Investigation, Writing – review & editing, Resources, Data curation, **Nicola Blake:** Investigation, Writing – review & editing, Resources, Data curation, **Wade Permar:** Investigation, Writing – review & editing, Resources, Data curation, **Lu Hu:** Investigation, Writing – review & editing, Funding acquisition, **Andrew Weinheimer:** Investigation, Resources, Data curation, **Geoff Tyndall:** Investigation, Writing – review & editing, Resources, Data curation, **Denise D. Montzka:** Investigation, Resources, Data curation, **Samuel R. Hall:** Investigation, Writing – review & editing, Resources, Data curation, **Kirk Ullmann:** Investigation, Writing – review & editing, Resources, Data curation, **Joel Thornton:** Investigation, Writing – review & editing, Funding acquisition, **Brett B. Palm:** Investigation, Writing – review & editing, Resources, Data curation, **Qiaoyun Peng:** Investigation, Writing – review & editing, Resources, Data curation, **Ilana Pollack:** Investigation, Writing – review & editing, Resources, Data curation, **Emily V. Fischer:** Conceptualization, Methodology, Validation, Investigation, Writing – original draft, Supervision, Project administration, Funding acquisition.

Declaration of competing interest

The authors declare that they have no known competing financial interests or personal relationships that could have appeared to influence the work reported in this paper.

Acknowledgements

Funding for this work was provided by the US National Science Foundation (NSF award numbers: AGS-1650786, AGS-1650275, and AGS-1652688). This material is based upon work supported by the National Center for Atmospheric Research, which is a major facility sponsored by the National Science Foundation under Cooperative Agreement No. 1852977. The data were collected using NSF's Lower Atmosphere Observing Facilities, which are managed and operated by NCAR's Earth Observing Laboratory. Additional support for the University of Washington was provided by the US National Oceanographic and Atmospheric Administration by award number NA17OAR4310012.

Appendix A. Supplementary data

Supplementary data to this article can be found online at <https://doi.org/10.1016/j.apr.2021.101269>.

References

Abatzoglou, J.T., Williams, A.P., 2016. Impact of anthropogenic climate change on wildfire across western US forests. *Proc. Natl. Acad. Sci. U.S.A.* 113, 11770–11775. <https://doi.org/10.1073/pnas.1607171113>.

Abeleira, A., Pollack, I.B., Sive, B., Zhou, Y., Fischer, E.V., Farmer, D.K., 2017. Source characterization of volatile organic compounds in the Colorado Northern Front Range Metropolitan Area during spring and summer 2015. *J. Geophys. Res.: Atmosphere* 122, 3595–3613. <https://doi.org/10.1002/2016JD026227>.

Akagi, S.K., Yokelson, R.J., Wiedinmyer, C., Alvarado, M.J., Reid, J.S., Karl, T., Crounse, J.D., Wennberg, P.O., 2011. Emission factors for open and domestic biomass burning for use in atmospheric models. *Atmos. Chem. Phys.* 11, 4039–4072. <https://doi.org/10.5194/acp-11-4039-2011>.

Alvarado, M.J., Logan, J.A., Mao, J., Apel, E., Riemer, D., Blake, D., Cohen, R.C., Min, K.-E., Perring, A.E., Browne, E.C., Woolridge, P.J., Diskin, G.S., Sachse, G.W., Fuelberg, H., Sessions, W.R., Harrigan, D.L., Huey, G., Liao, J., Case-Hanks, A., Jimenez, J.L., Cubison, M.J., Vay, S.A., Weinheimer, A.J., Knapp, D.J., Montzka, D. D., Flocke, F.M., Pollack, I.B., Wennberg, P.O., Kurten, A., Crounse, J., Clair, J.M.St, Wisthaler, A., Mikoviny, T., Yantosca, R.M., Carouge, C.C., Le Sager, P., 2010. Nitrogen oxides and PAN in plumes from boreal fires during ARCTAS-B and their impact on ozone: an integrated analysis of aircraft and satellite observations. *Atmos. Chem. Phys.* 10, 9739–9760. <https://doi.org/10.5194/acp-10-9739-2010>.

Apel, E.C., Hornbrook, R.S., Hills, A.J., Blake, N.J., Barth, M.C., Weinheimer, A., Cantrall, C., Rutledge, S.A., Basarab, B., Crawford, J., Diskin, G., Homeyer, C.R., Campos, T., Flocke, F., Fried, A., Blake, D.R., Brune, W., Pollack, I., Peischl, J., Ryerson, T., Wennberg, P.O., Crounse, J.D., Wisthaler, A., Mikoviny, T., Huey, G., Heikes, B., O'Sullivan, D., Riemer, D.D., 2015. Upper tropospheric ozone production from lightning NO_x-impacted convection: smoke ingestion case study from the DC3 campaign. *J. Geophys. Res.: Atmosphere* 120, 2505–2523. <https://doi.org/10.1002/2014JD022121>.

Atkinson, R., Baulch, D.L., Cox, R.A., Crowley, J.N., Hampson, R.F., Hynes, R.G., Jenkins, M.E., Rossi, M.J., Troe, J., Subcommittee, I.U.P.A.C., 2006. Evaluated kinetic and photochemical data for atmospheric chemistry. volume II – gas phase reactions of organic species. *Atmos. Chem. Phys.* 6, 3625–4055. <https://doi.org/10.5194/acp-6-3625-2006>.

Barry, K.R., Hill, T.C.J., Levin, E.J.T., Twohy, C.H., Moore, K.A., Weller, Z.D., Toohey, D. W., Reeves, M., Campos, T., Geiss, R., Schill, G.P., Fischer, E.V., Kreidenweis, S.M., DeMott, P.J., 2021. Observations of ice nucleating particles in the free troposphere from western US wildfires. *J. Geophys. Res.: Atmosphere* 126. <https://doi.org/10.1029/2020JD033752>.

Bian, Q., et al., 2019. A decadal climatology of chemical, physical, and optical properties of ambient smoke in the western and southeastern United States. *J. Geophys. Res. Atmos.* 125 (1) <https://doi.org/10.1029/2019JD031372> e2019JD031372.

Brewer, J.F., et al., 2019. Atmospheric photolysis of methyl ethyl, diethyl, and propyl ethyl ketones: Temperature-dependent UV absorption cross sections. *J. Geophys. Res. Atmos.* 124 (11), 5906–5918. <https://doi.org/10.1029/2019JD030391>.

Brey, S.J., Barnes, E.A., Pierce, J.R., Swann, A.L.S., Fischer, E.V., 2021. Past variance and future projections of the environmental conditions driving western U.S. Summertime wildfire burn area. *Earth's Future* 9. <https://doi.org/10.1029/2020EF001645>.

Brey, S.J., Ruminski, M., Atwood, S.A., Fischer, E.V., 2018. Connecting smoke plumes to sources using Hazard Mapping System (HMS) smoke and fire location data over North America. *Atmos. Chem. Phys.* 18, 1745–1761. <https://doi.org/10.5194/acp-18-1745-2018>.

Cazorla, M., Juncosa, J., 2018. Planetary boundary layer evolution over an equatorial Andean valley: a simplified model based on balloon-borne and surface measurements. *Atmos. Sci. Lett.* 19, e829. <https://doi.org/10.1002/asl.829>.

Ford, B., Martin, M.V., Zelasky, S.E., Fischer, E.V., Anenberg, S.C., Heald, C.L., Pierce, J. R., 2018. Future fire impacts on smoke concentrations, visibility, and health in the contiguous United States. *GeoHealth* 2, 229–247. <https://doi.org/10.1029/2018GH000144>.

Fowler, M., 2019. Wildfire smoke: trends, challenges, unknowns, and human response (master of science in civil engineering). Boise State University. <https://doi.org/10.18122/td/1521/poisestate>.

Garofalo, L.A., Pothier, M.A., Levin, E.J.T., Campos, T., Kreidenweis, S.M., Farmer, D.K., 2019. Emission and evolution of submicron organic aerosol in smoke from wildfires in the western United States. *ACS Earth Space Chem.* 3, 1237–1247. <https://doi.org/10.1021/acs.earthspacechem.9b00125>.

Gilman, J.B., et al., 2013. Source signature of volatile organic compounds from oil and natural gas operations in northeastern Colorado. *Environ. Sci. Technol.* 47 (3), 1297–1305. <https://doi.org/10.1021/es304119a>.

Gong, X., Kaulfus, A., Nair, U., Jaffe, D.A., 2017. Quantifying O₃ impacts in urban areas due to wildfires using a generalized additive model. *Environ. Sci. Technol.* 51, 13216–13223. <https://doi.org/10.1021/acs.est.7b03130>.

Gouw, J.A. de, Warneke, C., Parrish, D.D., Holloway, J.S., Trainer, M., Fehsenfeld, F.C., 2003. Emission sources and ocean uptake of acetonitrile (CH₃CN) in the atmosphere. *Journal of Geophysical Research: atmospheres* 108. <https://doi.org/10.1029/2002JD002897>.

Hall, S.R., Ullmann, K., Prather, M.J., Flynn, C.M., Murray, L.T., Fiore, A.M., Correa, G., Strode, S.A., Steenrod, S.D., Lamarque, J.-F., Guth, J., Josse, B., Flemming, J., Huijnen, V., Abraham, N.L., Archibald, A.T., 2018. Cloud impacts on photochemistry: building a climatology of photolysis rates from the Atmospheric Tomography mission. *Atmos. Chem. Phys.* 18, 16809–16828. <https://doi.org/10.5194/acp-18-16809-2018>.

Harvey, B.J., 2016. Human-caused climate change is now a key driver of forest fire activity in the western United States. *Proc. Natl. Acad. Sci. U.S.A.* 113, 11649–11650. <https://doi.org/10.1073/pnas.1612926113>.

Holloway, T., Levy, H., Kasibhatla, P., 2000. Global distribution of carbon monoxide. *J. Geophys. Res.* 105, 12123–12147. <https://doi.org/10.1029/1999JD901173>.

Huangfu, Y., Yuan, B., Wang, S., Wu, C., He, X., Qi, J., Gouw, J. de, Warneke, C., Gilman, J.B., Wisthaler, A., Karl, T., Graus, M., Jobson, B.T., Shao, M., 2021. Revisiting acetonitrile as tracer of biomass burning in anthropogenic-influenced environments. *Geophys. Res. Lett.* 48 <https://doi.org/10.1029/2020GL092322> e2020GL092322.

Jaffe, D.A., O'Neill, S.M., Larkin, N.K., Holder, A.L., Peterson, D.L., Halofsky, J.E., Rappold, A.G., 2020. Wildfire and prescribed burning impacts on air quality in the United States. *J. Air Waste Manag. Assoc.* 70, 583–615. <https://doi.org/10.1080/10962247.2020.1749731>.

Jaffe, D.A., Wigder, N.L., 2012. Ozone production from wildfires: a critical review. *Atmos. Environ.* 51, 1–10. <https://doi.org/10.1016/j.atmosenv.2011.11.063>.

Jost, C., Trentmann, J., Sprung, D., Andreae, M.O., McQuaid, J.B., Barjat, H., 2003. Trace gas chemistry in a young biomass burning plume over Namibia: observations and model simulations. *J. Geophys. Res.: Atmosphere* 108. <https://doi.org/10.1029/2002JD002431>.

Juncosa Calahorrano, J.F., Lindaas, J., O'Dell, K., Palm, B.B., Peng, Q., Flocke, F., Pollack, I.B., Garofalo, L.A., Farmer, D.K., Pierce, J.R., Collett, J.L., Weinheimer, A., Campos, T., Hornbrook, R.S., Hall, S.R., Ullmann, K., Pothier, M.A., Apel, E.C., Permar, W., Hu, L., Hills, A.J., Montzka, D., Tyndall, G., Thornton, J.A., Fischer, E. V., 2021. Daytime Oxidized Reactive Nitrogen Partitioning in Western U.S. Wildfire Smoke Plumes. *Journal of Geophysical Research: Atmosphere* 126. <https://doi.org/10.1029/2020JD033484> e2020JD033484.

Laing, J.R., Jaffe, D.A., 2019. Are causing extreme PM concentrations in the western United States 6.

Lebegue, B., et al., 2016. Comparison of nitrous oxide (N_2O) analyzers for high-precision measurements of atmospheric mole fractions. *Atmos. Meas. Tech.* 9 (3), 1221–1238. <https://doi.org/10.5194/amt-9-1221-2016>.

Lee, H.M., et al., 2014. Investigating the sensitivity of surface-level nitrate seasonality in Antarctica to primary sources using a global model. *Atmos. Environ.* 89, 757–767. <https://doi.org/10.1016/j.atmosenv.2014.03.003>.

Li, Q., Jacob, D.J., Bey, I., Yantosca, R.M., Zhao, Y., Kondo, Y., Notholt, J., 2000. Atmospheric hydrogen cyanide (HCN): biomass burning source, ocean sink? *Geophys. Res. Lett.* 27, 357–360. <https://doi.org/10.1029/1999GL010935>.

Li, Q., Jacob, D.J., Yantosca, R.M., Heald, C.L., Singh, H.B., Koike, M., Zhao, Y., Sachse, G.W., Streets, D.G., 2003. A global three-dimensional model analysis of the atmospheric budgets of HCN and CH3CN: constraints from aircraft and ground measurements. *J. Geophys. Res.: Atmosphere* 108. <https://doi.org/10.1029/2002JD003075>.

Lindaas, J., Pollack, I.B., Calahorrano, J.J., O'Dell, K., Garofalo, L.A., Pothier, M.A., Farmer, D.K., Kreidenweis, S.M., Campos, T., Flocke, F., Weinheimer, A.J., Montzka, D.D., Tyndall, G.S., Apel, E.C., Hills, A.J., Hornbrook, R.S., Palm, B.B., Peng, Q., Thornton, J.A., Permar, W., Wielgazs, C., Hu, L., Pierce, J.R., Collett, J.L., Sullivan, A.P., Fischer, E.V., 2021a. Empirical insights into the fate of ammonia in western U.S. Wildfire smoke plumes. *J. Geophys. Res.: Atmosphere* 126. <https://doi.org/10.1029/2020JD033730> e2020JD033730.

Lindaas, J., Pollack, I.B., Garofalo, L.A., Pothier, M.A., Farmer, D.K., Kreidenweis, S.M., Campos, T.L., Flocke, F., Weinheimer, A.J., Montzka, D.D., Tyndall, G.S., Palm, B.B., Peng, Q., Thornton, J.A., Permar, W., Wielgazs, C., Hu, L., Ottmar, R.D., Restaino, J. C., Hudak, A.T., Ku, I.-T., Zhou, Y., Sive, B.C., Sullivan, A., Collett, J.L., Fischer, E.V., 2021b. Emissions of reactive nitrogen from western U.S. Wildfires during summer 2018. *J. Geophys. Res.: Atmosphere* 126. <https://doi.org/10.1029/2020JD032657> e2020JD032657.

Liu, J.C., Mickley, L.J., Sulprizio, M.P., Dominici, F., Yue, X., Ebisu, K., Anderson, G.B., Khan, R.F.A., Bravo, M.A., Bell, M.L., 2016. Particulate air pollution from wildfires in the western US under climate change. *Climatic Change* 138, 655–666. <https://doi.org/10.1007/s10584-016-1762-6>.

Liu, X., Huey, L.G., Yokelson, R.J., Selimovic, V., Simpson, I.J., Müller, M., Jimenez, J.L., Campuzano-Jost, P., Beyersdorf, A.J., Blake, D.R., Butterfield, Z., Choi, Y., Crounse, J.D., Day, D.A., Diskin, G.S., Dubey, M.K., Fortner, E., Hanisco, T.F., Hu, W., King, L.E., Kleinman, L., Meinardi, S., Mikoviny, T., Onasch, T.B., Palm, B.B., Peischl, J., Pollack, I.B., Ryerson, T.B., Sachse, G.W., Sedlacek, A.J., Shilling, J.E., Springston, S., Clair, J.M.S., Tanner, D.J., Teng, A.P., Wennberg, P.O., Wisthaler, A., Wolfe, G.M., 2017. Airborne measurements of western U.S. wildfire emissions: comparison with prescribed burning and air quality implications. *J. Geophys. Res.: Atmosphere* 122, 6108–6129. <https://doi.org/10.1002/2016JD026315>.

Liu, X., Zhang, Y., Huey, L.G., Yokelson, R.J., Wang, Y., Jimenez, J.L., Campuzano-Jost, P., Beyersdorf, A.J., Blake, D.R., Choi, Y., Clair, J.M.S., Crounse, J.D., Day, D.A., Diskin, G.S., Fried, A., Hall, S.R., Hanisco, T.F., King, L.E., Meinardi, S., Mikoviny, T., Palm, B.B., Peischl, J., Perring, A.E., Pollack, I.B., Ryerson, T.B., Sachse, G., Schwarz, J.P., Simpson, I.J., Tanner, D.J., Thornhill, K.L., Ullmann, K., Weber, R.J., Wennberg, P.O., Wisthaler, A., Wolfe, G.M., Ziembka, L.D., 2016. Agricultural fires in the southeastern U.S. during SEAC4RS: emissions of trace gases and particles and evolution of ozone, reactive nitrogen, and organic aerosol. *J. Geophys. Res.: Atmosphere* 121, 7383–7414. <https://doi.org/10.1002/2016JD025040>.

Lu, X., Zhang, L., Yue, X., Zhang, J., Jaffe, D.A., Stohl, A., Zhao, Y., Shao, J., 2016. Wildfire influences on the variability and trend of summer surface ozone in the mountainous western United States. *Atmos. Chem. Phys.* 16, 14687–14702. <https://doi.org/10.5194/acp-16-14687-2016>.

Magzamen, S., Gan, R.W., Liu, J., O'Dell, K., Ford, B., Berg, K., Bol, K., Wilson, A., Fischer, E.V., Pierce, J.R., 2021. Differential cardiopulmonary health impacts of local and long-range transport of wildfire smoke. *GeoHealth* 5. <https://doi.org/10.1029/2020GH000330> e2020GH000330.

McClure, C.D., Jaffe, D.A., 2018a. Investigation of high ozone events due to wildfire smoke in an urban area. *Atmos. Environ.* 194, 146–157. <https://doi.org/10.1016/j.atmosenv.2018.09.021>.

McClure, C.D., Jaffe, D.A., 2018b. US particulate matter air quality improves except in wildfire-prone areas. *Proc. Natl. Acad. Sci. U.S.A.* 115, 7901–7906. <https://doi.org/10.1073/pnas.1804353115>.

Zheng, W., 2011. Characterization of a thermal decomposition chemical ionization mass spectrometer for the measurement of peroxy acyl nitrates (PANs) in the atmosphere. *Atmos. Chem. Phys.* 11 (13), 6529–6547. <https://doi.org/10.5194/acp-11-6529-2011>.

National Weather Service, n.d. Denver's Yearly/Monthly Extremes [WWW Document]. URL https://www.weather.gov/bou/Denver_Monthly_Extremes (accessed 7.22.21a).

O'Dell, K., Ford, B., Fischer, E.V., Pierce, J.R., 2019. Contribution of wildland-fire smoke to US PM 2.5 and its influence on recent trends. *Environ. Sci. Technol.* 53, 1797–1804. <https://doi.org/10.1021/acs.est.8b05430>.

O'Dell, K., Hornbrook, R.S., Permar, W., Levin, E.J.T., Garofalo, L.A., Apel, E.C., Blake, N.J., Jarnot, A., Pothier, M.A., Farmer, D.K., Hu, L., Campos, T., Ford, B., Pierce, J.R., Fischer, E.V., 2020. Hazardous air pollutants in fresh and aged western US wildfire smoke and implications for long-term exposure. *Environ. Sci. Technol.* 54, 11838–11847. <https://doi.org/10.1021/acs.est.0c04497>.

Palm, B.B., Peng, Q., Fredrickson, C.D., Lee, B.H., Garofalo, L.A., Pothier, M.A., Kreidenweis, S.M., Farmer, D.K., Pokhrel, R.P., Shen, Y., Murphy, S.M., Permar, W., Hu, L., Campos, T.L., Hall, S.R., Ullmann, K., Zhang, X., Flocke, F., Fischer, E.V., Thornton, J.A., 2020. Quantification of organic aerosol and brown carbon evolution in fresh wildfire plumes. *Proc. Natl. Acad. Sci. Unit. States Am.* 117, 29469–29477. <https://doi.org/10.1073/pnas.2012218117>.

Peng, Q., Palm, B.B., Melander, K.E., Lee, B.H., Hall, S.R., Ullmann, K., Campos, T., Weinheimer, A.J., Apel, E.C., Hornbrook, R.S., Hills, A.J., Montzka, D.D., Flocke, F., Hu, L., Permar, W., Wielgazs, C., Lindaas, J., Pollack, I.B., Fischer, E.V., Bertram, T. H., Thornton, J.A., 2020. HONO emissions from western U.S. Wildfires provide dominant radical source in fresh wildfire smoke. *Environ. Sci. Technol.* 54, 5954–5963. <https://doi.org/10.1021/acs.est.0c00126>.

Permar, W., Wang, Q., Selimovic, V., Wielgazs, C., Yokelson, R.J., Hornbrook, R.S., Hills, A.J., Apel, E.C., Ku, I.-T., Zhou, Y., Sive, B.C., Sullivan, A.P., Collett, J.L., Campos, T.L., Palm, B.B., Peng, Q., Thornton, J.A., Garofalo, L.A., Farmer, D.K., Kreidenweis, S.M., Levin, E.J.T., DeMott, P.J., Flocke, F., Fischer, E.V., Hu, L., 2021. Emissions of trace organic gases from western U.S. Wildfires based on WE-CAN aircraft measurements. *J. Geophys. Res.: Atmosphere* 126. <https://doi.org/10.1029/2020JD033838> e2020JD033838.

Pollack, I.B., et al., 2021. Weekend-weekday implications and the impact of wildfire smoke on ozone and its precursors at Boulder Reservoir, Colorado between 2017 and 2019. *J. Geophys. Res. Atmos.* 126 (17) <https://doi.org/10.1029/2021JD035221> e2021JD035221.

Pope, F.D., Smith, C.A., Davis, P.R., Shallcross, D.E., Ashfold, M.N.R., Orr-Ewing, A.J., 2005. Photochemistry of formaldehyde under tropospheric conditions. *Faraday Discuss.* 130, 59–72. <https://doi.org/10.1039/B419227C>.

Ridley, B.A., et al., 1992. A small high-sensitivity, medium-response ozone detector suitable for measurements from light aircraft. *J. Atmos. Ocean. Technol.* 9 (2), 142–148. [https://doi.org/10.1175/1520-0426\(1992\)009<0142:ASHSMR>2.0.CO;2](https://doi.org/10.1175/1520-0426(1992)009<0142:ASHSMR>2.0.CO;2).

Ridley, B.A., Graheck, F.E., 1990. A small, low flow, high sensitivity reaction vessel for NO chemiluminescence detectors. *J. Atmos. Ocean. Technol.* 7 (2), 307–311. [https://doi.org/10.1175/1520-0426\(1990\)007<0307:ASLFHS>2.0.CO;2](https://doi.org/10.1175/1520-0426(1990)007<0307:ASLFHS>2.0.CO;2).

Rolph, G.D., Draxler, R.R., Stein, A.F., Taylor, A., Ruminski, M.G., Kondragunta, S., Zeng, J., Huang, H.-C., Manikin, G., McQueen, J.T., Davidson, P.M., 2009. Description and verification of the NOAA smoke forecasting System: the 2007 fire season. *Weather Forecast.* 24, 361–378. <https://doi.org/10.1175/2008WAF2221651>.

Ruminski, M., Kondragunta, S., Draxler, R., Zeng, J., 2006. Recent changes to the hazard mapping System.

Sander, S.P., Golden, D.M., Kurylo, M.J., Moortgat, G.K., Wine, P.H., Ravishankara, A.R., Kolb, C.E., Molina, M.J., Finlayson-Pitts, B.J., Huie, R.E., Orkin, V.L., Friedl, R.R., Keller-Rudek, H., 2006. Chemical Kinetics and Photochemical Data for Use in Atmospheric Studies : Evaluation Number 15 (Technical Report). Jet Propulsion Laboratory, California Institute of Technology, Pasadena, CA.

Singh, H.B., Anderson, B.E., Brune, W.H., Cai, C., Cohen, R.C., Crawford, J.H., Cubison, M.J., Czech, E.P., Emmons, L., Fuelberg, H.E., 2010. Pollution influences on atmospheric composition and chemistry at high northern latitudes: boreal and California forest fire emissions. *Atmos. Environ.* 44, 4553–4564. <https://doi.org/10.1016/j.atmosenv.2010.08.026>.

Slusher, D.L., et al., 2004. A thermal dissociation–chemical ionization mass spectrometry (TD-CIMS) technique for the simultaneous measurement of peroxyacetyl nitrates and dinitrogen pentoxide. *J. Geophys. Res. Atmos.* 109 (D19) <https://doi.org/10.1029/2004JD004670>.

Strum, M., Scheffe, R., 2016. National review of ambient air toxics observations. *J. Air Waste Manag. Assoc.* 66, 120–133. <https://doi.org/10.1080/10962247.2015.1076538>.

Trentmann, J., Andreae, M.O., Graf, H.-F., 2003. Chemical processes in a young biomass-burning plume. *J. Geophys. Res.: Atmosphere* 108. <https://doi.org/10.1029/2003JD003732>.

Val Martin, M., Heald, C.L., Lamarque, J.-F., Tilmes, S., Emmons, L.K., Schichtel, B.A., 2015. How emissions, climate, and land use change will impact mid-century air quality over the United States: a focus on effects at national parks. *Atmos. Chem. Phys.* 15, 2805–2823. <https://doi.org/10.5194/acp-15-2805-2015>.

van der Werf, G.R., Randerson, J.T., Giglio, L., van Leeuwen, T.T., Chen, Y., Rogers, B.M., Mu, M., van Marle, M.J.E., Morton, D.C., Collatz, G.J., Yokelson, R.J., Kasibhatla, P. S., 2017. Global fire emissions estimates during 1997–2016. *Earth Syst. Sci. Data* 9, 697–720. <https://doi.org/10.5194/essd-9-697-2017>.

WE-CAN | Earth Observing Laboratory [WWW Document], n.d. URL https://www.eol.ucar.edu/field_projects/we-can (accessed 8.5.21).

Wentworth, G.R., Aklilu, Y., Landis, M.S., Hsu, Y.-M., 2018. Impacts of a large boreal wildfire on ground level atmospheric concentrations of PAHs, VOCs and ozone. *Atmos. Environ.* 178, 19–30. <https://doi.org/10.1016/j.atmosenv.2018.01.013>.

Wiedinmyer, C., Quayle, B., Geron, C., Belote, A., McKenzie, D., Zhang, X., O'Neill, S., Wynne, K.K., 2006. Estimating emissions from fires in North America for air quality

modeling. *Atmos. Environ.* 40, 3419–3432. <https://doi.org/10.1016/j.atmosenv.2006.02.010>.

Yokelson, R.J., Crounse, J.D., DeCarlo, P.F., Karl, T., Urbanski, S., Atlas, E., Campos, T., Shinozuka, Y., Kapustin, V., Clarke, A.D., Weinheimer, A., Knapp, D.J., Montzka, D., Holloway, J., Weibring, P., Flocke, F., Zheng, W., Toohey, D., Wennberg, P.O., Wiedinmyer, C., Mauldin, L., Fried, A., Richter, D., Walega, J., Jimenez, J.L., Adachi, K., Buseck, P.R., Hall, S.R., Shetter, R., 2009. Emissions from biomass burning in the Yucatan. *Atmos. Chem. Phys.* 9, 5785–5795.

Yue, X., Mickley, L.J., Logan, J.A., Kaplan, J.O., 2013. Ensemble projections of wildfire activity and carbonaceous aerosol concentrations over the western United States in the mid-21st century. *Atmos. Environ.* 77, 767–780. <https://doi.org/10.1016/j.atmosenv.2013.06.003>.